Title

Oral infection of mice with Fusobacterium nucleatum results in macrophage recruitment to the dental pulp and bone resorption.

Journal

Biomedical journal, 41(3)

ISSN

2319-4170

Authors

Johnson, Larry
Almeida-da-Silva, Cássio Luiz Coutinho
Takiya, Christina Maeda
et al.

Publication Date

2018-06-01

DOI

10.1016/j.bj.2018.05.001

Peer reviewed

Available online at www.sciencedirect.com

ScienceDirect

Biomedical Journal

journal homepage: www.elsevier.com/locate/bj

Original Article

Oral infection of mice with *Fusobacterium nucleatum* results in macrophage recruitment to the dental pulp and bone resorption

Larry Johnson [a,b], *Cássio Luiz Coutinho Almeida-da-Silva* [a,b], *Christina Maeda Takiya* [b], *Vanessa Figliuolo* [b], *Gustavo Miranda Rocha* [c], *Gilberto Weissmüller* [c], *Julio Scharfstein* [b], *Robson Coutinho-Silva* [b,1], *David M. Ojcius* [a,b,*,1]

[a] *Department of Biomedical Sciences, University of the Pacific, Arthur Dugoni School of Dentistry, San Francisco, CA, USA*

[b] *Immunobiology Program, Institute of Biophysics Carlos Chagas Filho, Federal University of Rio de Janeiro, Rio de Janeiro, Brazil*

[c] *Molecular and Structural Biology Program, Institute of Biophysics Carlos Chagas Filho, Federal University of Rio de Janeiro, Rio de Janeiro, Brazil*

ARTICLE INFO

Article history:
Received 24 December 2017
Accepted 8 May 2018
Available online 2 July 2018

Keywords:
Immunology
Inflammation
Periodontal disease
Dental
Innate immunity

ABSTRACT

Background: *Fusobacterium nucleatum* is a Gram-negative anaerobic bacterium associated with periodontal disease. Some oral bacteria, like *Porphyromonas gingivalis*, evade the host immune response by inhibiting inflammation. On the other hand, *F. nucleatum* triggers inflammasome activation and release of danger-associated molecular patterns (DAMPs) in infected gingival epithelial cells.

Methods: In this study, we characterized the pro-inflammatory response to *F. nucleatum* oral infection in BALB/c mice. Western blots and ELISA were used to measure cytokine and DAMP (HMGB1) levels in the oral cavity after infection. Histology and flow cytometry were used to observe recruitment of immune cells to infected tissue and pathology.

Results: Our results show increased expression and production of pro-inflammatory cytokines during infection. Furthermore, we observe that *F. nucleatum* infection leads to recruitment of macrophages in different tissues of the oral cavity. Infection also contributes to osteoclast recruitment, which could be involved in the observed bone resorption.

Conclusions: Overall, our findings suggest that *F. nucleatum* infection rapidly induces inflammation, release of DAMPs, and macrophage infiltration in gingival tissues and suggest that osteoclasts may drive bone resorption at early stages of the inflammatory process.

* *Corresponding author*. Department of Biomedical Sciences, University of the Pacific, Arthur Dugoni School of Dentistry, 155 Fifth St., San Francisco, CA 94103, USA.
E-mail address: dojcius@pacific.edu (D.M. Ojcius).

Peer review under responsibility of Chang Gung University.

[1] These authors share senior co-authorship.

https://doi.org/10.1016/j.bj.2018.05.001

At a glance commentary

Scientific background on the subject

The effect of *Fusobacterium nucleatum* on the immune response remains poorly understood in mouse models of oral infection.

What this study adds to the field

This study showed that oral infection with *F. nucleatum* stimulates inflammation and infiltration of macrophages in gingival tissue, which could lead to bone loss in the oral cavity.

The oral cavity is colonized with hundreds of different species of bacteria which compose the oral microbiome [1,2]. Some common bacteria found in individuals afflicted with periodontitis include *Fusobacterium nucleatum*, *Porphyromonas gingivalis*, and *Aggregatibacter actinomycetemcomitans* [3,4]. Gingivitis is diagnosed when the gingiva, or gums, reveals signs of swelling, redness, or chronic bleeding [5], usually associated with gingival infection. However, chronic inflammation can lead to development of periodontitis with signs of deep periodontal pockets, alveolar bone resorption, and tooth loss [6,7].

The tooth is surrounded by the gingival epithelium. This microenvironment is optimal for growth of anaerobic bacteria and provides an opportunity for pathogenic bacteria to attach and coaggregate into biofilms [8]. *F. nucleatum* is one of the predominant bacteria and contributors to biofilm formation [9–11]. The bacteria utilize adhesion mechanisms of lectin-like and non-lectin-like interactions and adhesion peptides, such as FadA (*Fusobacterium* adhesin A) for attachment [12–16]. These interactions facilitate coaggregation or infiltration into lymphocytes, polymorphonuclear neutrophils, erythrocytes, epithelial cells, and fibroblasts [11,12,14,17,18].

The oral epithelium defends against bacterial colonization by secretion of antimicrobial peptides called defensins [4,19–21]. β-defensins target bacteria as the peptides are electrostatically attracted to their negative charged membranes and induce pore formation [4,19,22]. Antimicrobial peptides can also act as chemoattractants and recruit other immune cells, neutrophils or T cells [4,7,19]. Thus, β-defensins play an active role as part of innate and adaptive responses to oral infection.

Gingival epithelial cells (GECs) represent a major barrier to infection by invasive bacteria, and also contribute to immune recognition of the pathogens and the immune response [23,24]. When pathogen-associated molecular patterns (PAMPs) of bacteria are recognized by host pathogen recognition receptors (PRRs) on GECs, they activate NF-κB and induce expression of cytokines and chemokines, and recruit neutrophils and macrophages [25–27]. Recognition of *F. nucleatum* and *A. actinomycetemcomitans* infection results in production of cytokines such as IL-1β [28–30]. TNF-α and IL-17 can also synergize with IL-1β to enhance expression and production of other cytokines (e.g., IL-6) and defensins, along with endothelial activation to enhance the immune response [31–36].

Although the goal of inflammation is to resolve oral infection, it can also lead to bone resorption. Alveolar bone is one of the most dynamic bones in the body, as osteoclasts and osteoblasts continually induce bone remodeling to maintain homeostasis [37–40]. Osteoclasts are resorptive cells that are activated and differentiated by macrophage-colony stimulating factor, receptor activator of nuclear factor kappa-B ligand (RANKL)-RANK signaling, interleukins, and TNF-α [38,39,41–43]. Once osteoclasts adhere to bone, a ruffled border is created between the activated osteoclast and bone [38,40], and osteoclasts are able to degrade the mineral matrix [38,40]. Degraded bone matrix is removed as it is transcytosed in vesicles through osteoclasts, and fuses with cytoplasmic vesicles containing tartrate-resistant acid phosphatase (TRAP) to be released in the extracellular matrix [38,44]. Phagocytes remove the debris and osteoblasts are recruited for bone formation after osteoclasts detach from the bone [38].

F. nucleatum mechanisms for invasion and host response have been evaluated both *in vitro* and *in vivo* [3,45–48]. We have previously reported that *F. nucleatum* infection induces inflammasome activation and release of cytokines and danger signals in human GECs *in vitro* [29,46]. In this study, we examined the immune response to *F. nucleatum* oral infection in BALB/c mice, which had not been previously characterized.

Materials and methods

Bacteria

F. nucleatum (ATCC 25586) was cultured at 37 °C under anaerobic conditions in brain-heart infusion broth supplemented with yeast extract (5 mg/mL), hemin (5 μg/mL), and menadione (1 μg/mL). Erythromycin (5 μg/ml) was used as a selective agent for *F. nucleatum* as previously described [49]. After 24 h of growth, bacteria were collected by centrifugation at 6000 × *g* for 10 min at 4 °C, washed twice and resuspended with phosphate-buffered saline (PBS). Quantification of bacteria was measured by optical density (OD) to obtain a concentration of 10^9 colony-forming units (CFU)/ml using a reference standard.

Mice and oral challenge with F. nucleatum

BALB/c mice were obtained from the animal facility of the Institute of Biophysics Carlos Chagas Filho at the Federal University of Rio de Janeiro. All protocols used in this study followed the guidelines and were approved by the Institutional Animal Care and Use Committee at the Federal University of Rio de Janeiro (CEUA-UFRJ 076/15).

Six-to eight-week-old male BALB/c mice were given ad libitum water containing 10 mL of Bactrim (Roche) comprised of sulfamethoxazole/trimethoprim for 10 days. Then antibiotic-free water was given to the mice for 3 days prior to infection. The protocol for oral infection was adapted from Baker et al. [50]. On days of infection, mice were anesthetized with 100 μl of ketamine-xylazine solution (100 mg/ml and 20 mg/ml) by intraperitoneal injection. Anesthetized mice

were orally challenged with *F. nucleatum* at 10^9 bacteria in 100 μl of PBS with 2% carboxymethylcellulose (Sigma), or were sham-infected with the same solution containing no bacteria three times over 2-day intervals.

Collection of maxilla

Maxillas were surgically removed collected at days 1, 4, and 7 after the last infection day. Half maxilla was placed in TRIzol reagent (Life Technologies) for PCR analysis and the other half in cell lysis buffer (Sigma) containing protease inhibitor (Roche) for western blotting analysis. Then the samples were macerated and homogenized using TissueLyser LT (Qiagen) for 5 min at 50 Hz. After centrifugation at 1000 × *g* for 10 min supernatants were transferred to new tubes and used for experiments. Prior to protein assays, maxilla halves from each group of mice were pooled together and quantified using Pierce BCA Protein Assay Kit (Thermo Fisher Scientific) for equal loading.

Isolation, processing and analysis of murine gingival cells

The isolation, processing and analysis of murine maxilla gingival cells collected from uninfected or *F. nucleatum*-infected mice was as described by Mizraji et al., 2013 [51]. Briefly, after the protocol for oral infection, mice were euthanized and both upper and lower mandibles were collected. The mandibles were cut into hemi-maxillae and the palatal tissue was trimmed until reaching the alveolar bone. Gingival tissues were peeled using forceps (without teeth), placed in 1 ml PBS + 2% FCS, 2 mg/mL of collagenase type II and 1 mg/mL of DNAse type 1, well minced and incubated in a shaker incubator for 20 min at 37 °C, 200 rpm, plus an additional 10 min after adding 20 μl of EDTA 0.5 M. Samples were washed with 12 ml of PBS + 2% FCS and centrifuged at 4 °C, 400 × *g* for 8 min. Cells were resuspended with 2 ml PBS + 2% FCS and filtered on a 70 μm cell-strainer. The collected samples were centrifuged at 4 °C, 320 × *g* for 5 min and resuspended with 300 μL PBS + 2% FCS for cellular quantification and antibody staining.

Flow cytometry analysis

Freshly isolated murine gingival cells were immunostained for flow cytometry analysis. 5×10^5 cells were stained with 0.1 μg/mL Fixable Viability Stain 510 (FVS510) – BD Horizon™ for 15 min at room temperature to distinguish live and dead cells. After washing with PBS, cells were blocked for nonspecific binding with 5 μg/mL with CD16/32 mAb for 20 min on ice and stained with the following monoclonal antibodies (eBioscience) for 30 min at 4 °C: 1 μg/mL anti-CD90 (Thy-1.2) APC (Clone 53–2.1), 1 μg/mL anti- F4/80 Antigen eFluor® 450 (Clone BM8), 1 μg/mL anti-Ly-6G PE (clone 1A8-Ly6g), 2.5 μg/mL anti-CD11b Alexa Fluor® 488 (Clone M1/70). Cells were washed with PBS, fixed with 4% paraformaldehyde for 20 min at room temperature and kept at PBS until their acquisition by flow cytometry. Fluorescence was evaluated by acquiring 50,000 events/sample using FACSCanto II (BD Biosciences, San Jose, California, USA). Results were analyzed using the FACSDiva (BD Biosciences, San Jose, California, USA) and presented as percentage of positive events.

RNA extraction and quantitative PCR

Following the manufacturer's instructions, total RNA was extracted using Trizol Reagent (Life Technologies). Total RNA was quantified by using NanoDrop (Thermo Fisher Scientific). RNA was converted to cDNA using High-Capacity cDNA Reverse Transcription Kit (Life Technologies). Quantitative PCR was performed using SYBR-green fluorescence quantification system (SYBR Select Master Mix (Life Technologies)). Real-time PCR cycling parameters were as follows: 95 °C for 10 min and then 40 cycles of 95 °C for 30 s, 60 °C for 1 min, and 72 °C for 1 min. The following primers were used as previously described: IL-1β forward, 5′-TTCAGGCAGGCAGTATCACTC-3′; IL-1β reverse, 5′-CCACGGGAAAGACACAGGTAG-3′; TNFα forward, 5′-TTCTATG GCCCAGACCCTCA-3′; TNFα reverse, 5′-GTGGTTTGCTACG ACGTGGG-3′; IL-6 forward, 5′-TCCTCTCTGCAAGAGACTTCC-3′; IL-6 reverse, 5′-TTGTGAAGTAGGGAAGGCCG-3′; IL-17 forward, 5′-TCAGCGTGTCCAAACACTGAG-3′, IL-17 reverse, 5′-GACTTT-GAGGTTGACCTTCACAT-3′; GAPDH forward, 5′-GGTCATCCCA-GAGCTGAACG-3′; GAPDH reverse, 5′- TTGCTGTTGAAG TCGCAGGA-3′ [52]. Relative expression levels were calculated against GAPDH as the reference gene using the comparative cycle threshold method. Quantification of infected mice results were normalized against control mice.

PCR

The PCR was performed following the protocol from Liu et al. [53]. Maxilla RNA targeted a 360-bp region using *F. nucleatum* forward, 5′-AGAGTTTGATCCTGGCTCAG-3′ and reverse, 5′-GTCATCGTGCACACAGAATTGCTG-3′ primer sequences [53]. The samples were amplified using GoTaq Green Master Mix (Promega) under the same conditions of 5 min at 94 °C and 30 cycles, with each cycle consisting of denaturation at 94 °C for 30 s, annealing at 58 °C for 30 s, extension at 72 °C for 1 min, and final extension for 10 min. PCR products were loaded onto a 2% gel in Tris-acetate buffer with EDTA. The gel was stained with GelRed nucleic acid gel stain (Biotium) and visualized under UV light.

ELISA

Homogenized maxilla were used for ELISA experiments. IL-1β, IFN-γ, and TNF-α cytokine levels were measured using Mouse IL-1β, IFN-γ, and TNF-α ELISA kits (R&D Systems). ELISAs were performed following manufacturer's instructions.

Western blot

Protein samples were dissolved in 6X Laemmli buffer and boiled. Then they were run on SDS-PAGE gels and transferred to PVDF membranes. Membranes were blocked with 5% BSA and incubated with anti-HMGB1 (Abcam) overnight. After primary incubation, the membranes were washed and incubated with HRP conjugated anti-goat IgG antibody (Millipore). Finally, the membranes were developed with Luminata Forte (Millipore) substrate. Images were acquired using ImageQuant LAS 4000 system and analyzed using NIH-ImageJ.

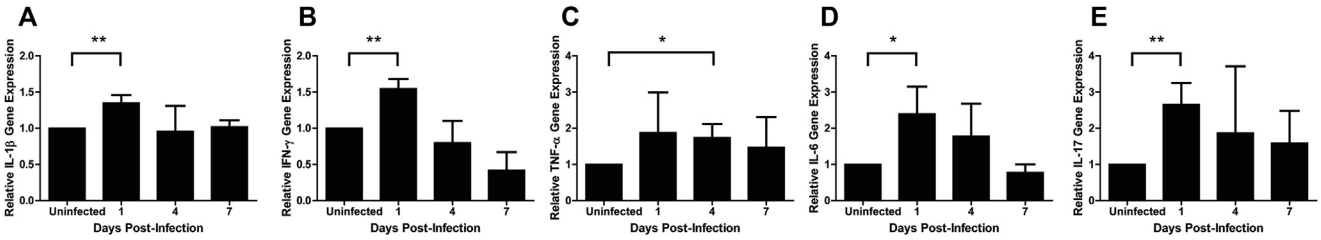

Fig. 1 **Gene expression is upregulated in the maxilla during *F. nucleatum* infection**. (A–E) Relative IL-1β, IFN-γ, TNF-α, IL-6, and IL-17 mRNA gene expression compared with control was evaluated by real-time PCR (qPCR) from the maxilla of *F. nucleatum* infected BALB/c mice. Days 1, 4, and 7 post-infection were tested. Results represent an average of three independent experiments with at least 4 mice in each group per experiment. Error bars represent the mean ± SD. (*< 0.05, **<0.01, Student's *t*-test).

Histopathology and immunohistochemistry

For morphological studies mandibles were collected and were immediately immersed in zinc-formaldehyde for fixation for 72 h. Next, tissues were decalcified in Morse's solution for 7 days. The complete decalcification of bones was manually assessed. Tissues were then washed in water and dehydrated crescent solutions of ethanol, clarified in xylene and embedded in paraffin. Five-micrometer sections were cut and stained with hematoxylin-eosin (H&E). For immunohistochemistry, paraffin sections were collected onto charged histological slides. A rat monoclonal antibody F4/80 (Abd Serotec) was used to detect macrophages. Briefly, after dewaxing and rehydrating, sections were submitted to endogenous peroxidase inhibition (15 min with 3% H_2O_2 in methanol), followed by an enzymatic antigen retrieval, with a 0.1% trypsin solution containing 0.01% calcium chloride in Tris-buffer pH 7.4 (Sigma-Aldrich) for 5 min. After blocking nonspecific binding of immunoglobulins, primary antibody was incubated for 14–18 h, at 4 °C, in a humid chamber. The sections were then washed in 0.25% Tween-phosphate saline buffer (PBS) solution for 5 min and then the secondary antibody conjugated to peroxidase were incubated for 1 h at room temperature (Nichirei). The chromogen substrate was diaminobenzidine (Dako). Negative control slides were incubated with rat nonimmune serum or with the antibody diluent solution.

Histomorphometry

Histomorphometry was performed using a computer-assisted image analysis system comprising a Nikon Eclipse E-800 microscope connected *via* a digital camera (Evolution, Media Cybernetics Inc., Bethesda, MD) to a computer. The graphical interface software Q-Capture 2.95.0, version 2.0.5 (Silicon Graphic Inc., Milpitas, CA) was used. Ten high quality photomicrographs (high-quality images, 2048 × 1536 pixel buffer) were randomly captured from tissues of each animal using the 40× objective lens.

Quantification of the number of F4/80 macrophages

The number of macrophages was quantified in F4/80-stained sections. Results were expressed as the number of macrophages/histological field.

AFM force spectroscopy

For force spectroscopy studies, uninfected and 1, 4 and 7 days infected mandibles were collected and immediately immersed in PBS. After, tissues were cleaned, and the region of alveolar bone was exposed to start the measurement. Bone region was examined in a Dimension Icon Scanning Probe Microscopy (Bruker, Santa Barbara – CA). RTESPA-300 AFM probe (Bruker, Camarillo – CA) was used and its cantilever elastic constant was obtained by thermal noise method. Force curves were acquired in air using contact mode and young modulus elasticity was extracted by those curves using NanoScope Analysis 1.5 software (Bruker, Santa Barbara – CA).

Statistical analysis

Results are shown as mean ± standard deviation (SD). Statistical significance was calculated by two-tailed Student's *t*-test and differences were considered significant at $P < 0.05$.

SPM results were evaluated by one-way Anova followed by Dunnett's test and differences were considered significant at $p < 0.05$.

Results

F. nucleatum *infection induced pro-inflammatory cytokine expression in maxilla*

To assess cytokine expression in *F. nucleatum*-infected mice, we isolated RNA from the maxilla at various time points post-infection. Since *F. nucleatum* infection in GECs led to a time-dependent increase of IL-1β gene expression *in vitro* [46], we determined whether oral infection of *F. nucleatum* in mice would similarly upregulate IL-1β gene expression over a course of 7 d.p.i. (days post infection) [Fig. 1A]. Indeed, we observed a significant induction of IL-1β 1 d.p.i. compared to uninfected mice followed by a decrease in the transcriptional response thereafter. Because it was already known that *F. nucleatum*-infected BMDMs trigger cytokine production (such as IL-1β, TNF-α, and IL-6) through the Toll-like receptor (TLR) signaling pathway [54], we analyzed mRNA expression of other pro-inflammatory cytokines in our *in vivo* model of *F. nucleatum* infection. IFN-γ and IL-6 mRNA expression followed the same time-dependent response

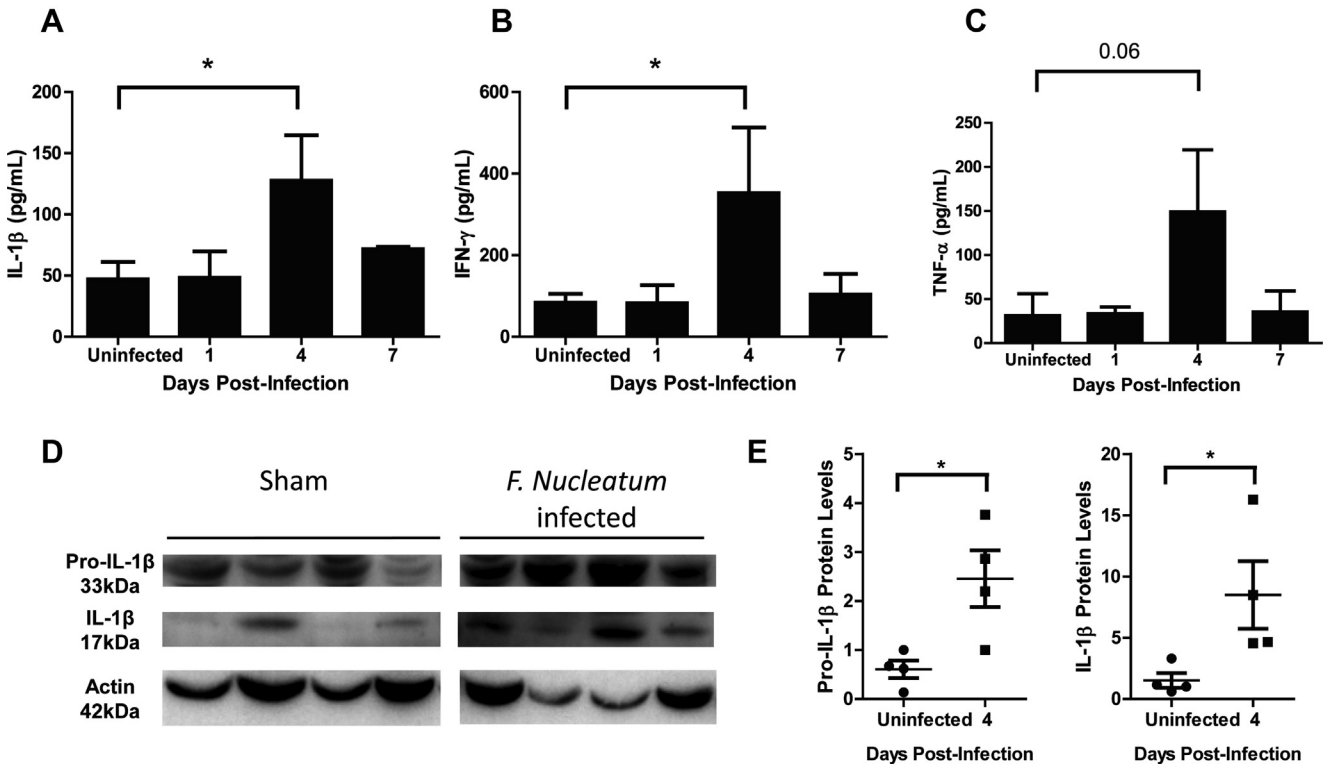

Fig. 2 ***F. nucleatum* infection induces increased cytokine production in the maxilla**. (A–C) The cytokines IL-1β, IFN-γ, and TNF-α were measured by ELISA. Maxilla from days 1, 4, and 7 post-infection with *F. nucleatum* were evaluated. (D) Western blotting to evaluate immature pro-IL-1β (33 kDa) and mature IL-1β (17 kDa) protein expression from the maxilla of *F. nucleatum*-infected BALB/c mice at day 4. Actin (42 kDa) was used as a loading control. (E) Relative protein was measured by quantification of densitometry using NIH-ImageJ. (A–C) represent an average of three independent experiments with at least 4 mice in each group per experiment. (D and E) represent average of 4 mice in each group. Error bars represent the mean ± SD. (*< 0.05, **<0.01, Student's *t*-test).

described for IL-1β, with an increase of gene expression at 1 d.p.i., decreasing thereafter [Fig. 1B and D]. On the other hand, TNF-α enhancement was delayed (at 4 d.p.i) but also declined thereafter [Fig. 1C]. Since IL-17 is implicated in bone resorption [52–55], we examine its transcriptional response and found that it was upregulated early during infection, at 1 d.p.i., as observed for IL-1β, IFN-γ and IL-6 [Fig. 1E]. The results indicated that multiple pro-inflammatory cytokines were upregulated during the course of *F. nucleatum* infection.

Cytokine production is enhanced in the maxilla during F. nucleatum *infection*

To directly evaluate cytokine production, we performed ELISA analysis using maxilla samples of infected mice and found that IL-1β and IFN-γ levels increased at 4 d.p.i.; i.e., 3 d after the transcriptional activation of these genes [Fig. 2A and B]. Additionally, a slight (non-statistically significant) increase of TNF-α was noted at 4 d pi [Fig. 2C].

To further analyze the cytokine production, we determined by Western blotting the presence of the immature and mature forms of IL-1β in the maxilla of mice at the peak of cytokine production (4 d.p.i.). There was an enhancement of pro-IL-1β and IL-1β protein expression in the maxilla of *F. nucleatum*-infected mice, compared with sham-infected mice [Fig. 2D]. Confirmed by densitometry analysis [Fig. 2E], these data suggest that the early (1 d.p.i.) transcriptional response induced by *F. nucleatum* translated into sustained production of the pro-IL-1β precursor, which underwent cleavage at this time-point (4 d.p.i.). These *in vivo* results are consistent with our previous findings showing that IL-1β production by *F. nucleatum*-infected GECs is driven by the NRLP3 inflammasome-caspase 1 pathway [29].

Next, we looked at high mobility group box 1 (HMGB1) expression because this damage-associated motif pattern (DAMP) acts as a transcription regulator, pro-inflammatory cytokine, and macrophage activator [55–57]. IFN-γ, TNF-α, and TGF-β have been shown to augment expression of HMGB1 mRNA in THP-1 macrophages and human peripheral-blood monocytes [56,58]. As we observed an increase in two of these cytokines during *F. nucleatum* oral infection, it seemed plausible that these pro-inflammatory responses were linked to HMGB1 production. Using Western blot analysis, we found a significant increase of HMGB1 expression at 4 d.p.i. as compared with the sham-infected mice [Fig. 3A and B].

F. nucleatum *infection results in recruitment of immune cells to the maxilla*

Given that inflammatory cytokine production is increased over time in *F. nucleatum* infected mice, we next characterized the dynamics of leukocyte infiltration in tissue sections

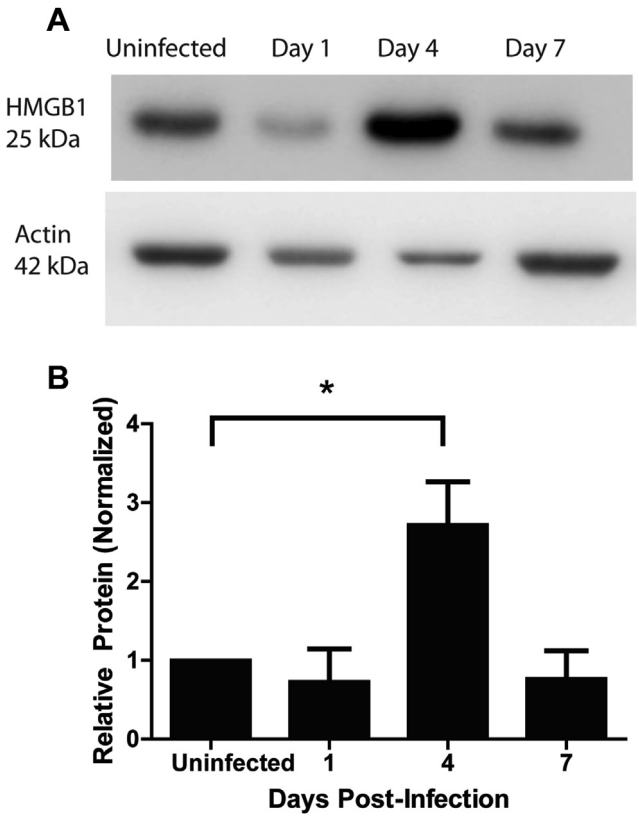

Fig. 3 **HMGB1 levels augmented at day 4 post-infection**. (A) HMGB1 (25 kDa) was detected by Western blot from the maxilla of BALB/c mice infected with *F. nucleatum* over a time-course of day 1, 4, and 7 post-infection. Actin (42 kDa) was used as a loading control. (B) Relative protein was measured by quantification of densitometry using NIH-ImageJ. Results represent an average of three independent experiments with at least 4 mice in each group per experiment. Error bars represent the mean ± SD. (*< 0.05 Student's *t*-test).

obtained from the mandible. Analysis by H&E showed increased numbers of infiltrating leukocytes near the alveolar bone at 1, 4 and 7 d.p.i., when compared with uninfected mice [Fig. 4A]. To confirm this result, we quantified total inflammatory cells isolated from murine gingival tissues surrounding the teeth and found increased infiltration at 4 d.p.i. as compared with the uninfected group [Fig. 4B].

To further characterize the infiltrated cells after *F. nucleatum* infection *in vivo*, we used immunohistochemistry images to observe macrophage infiltration of the infected gingival tissues. F4/80$^+$ staining revealed that macrophage recruitment is increased in the infected gingiva (1 and 7 d.p.i.) when compared with uninfected mice [Fig. 5A and B]. We next quantified CD11b$^+$ Ly6G$^+$ neutrophils [Fig. 5C] and CD90 + lymphocytes [Fig. 5D] and found a modest increase (not statistically significant) in both subsets in the infected mice group compared to controls [59]. Activated macrophages were detected in adipose tissues, skeletal muscle fibers, and periosteal localization [59]. Noteworthy, however, macrophages were more concentrated in the dental pulp, around the periodontal ligaments, and also between odontoblasts.

Bone resorption during F. nucleatum *infection*

Osteoclast activation leads to their attachment to the bone, resorption of the bone through its secretory factors, and detachment from the resorption site [60,61]. Previous studies have shown that IL-1β, and TNF-α enhance osteoclast development [41,62,63]. Since the production of these cytokines was elevated during *F. nucleatum* infection, we determined whether these inflammatory responses were coupled to bone resorption by osteoclasts. Indeed, we detected bone resorption pits in the alveolar bone (7 d.p.i.) compared to the uninfected group [Fig. 6], which may have resulted from osteoclast involvement.

F. nucleatum *infection is associated with softened alveolar bone*

To analyze the impact of the infection on bone structure, we measured the mechanical properties of the alveolar bone by Force Spectroscopy using an atomic force microscope. Uninfected mice prepared for these experiments expressed an elastic constant average of 7.95 ± 10.73 GPa [Fig. 7]. Infected mice had a significantly lower elasticity when compared with uninfected mice. These differences were more obvious between uninfected and infected mice 1 d.p.i, when elasticity decreased to 2.76 ± 5.56 GPa. Elasticity values at days 4 and 7 were 5.61 ± 7.88 GPa and 3.44 ± 3.42 GPa, respectively [Fig. 7].

Discussion

Previous studies have examined the mechanisms involved in the adhesion and metabolic growth interactions between *F. nucleatum* and other periodontal bacteria, such as *P. gingivalis* and *A. actinomycetemcomitans* [64–67], but monomicrobial oral infection with *F. nucleatum* in BALB/c mice had never been reported.

Our studies demonstrated that *F. nucleatum* can rapidly trigger inflammatory responses, manifested as increased mRNA for pro-inflammatory cytokines such as IL-1β, IFN-γ, IL-6 and IL-17 at 1 d.p.i., and secreted high levels of IL-1β and IFN-γ and the DAMP, HMGB1, in the maxilla at 4 d.p.i. These effects were followed by immune cell infiltration in gingival tissue observed from 1 d.p.i. on, culminating in bone resorption detected as early as 7 d.p.i. Alveolar bone softness was detected soon after, at 1 d.p.i.

Different oral bacteria can negatively or positively regulate the production of pro-inflammatory cytokines in GECs. While *P. gingivalis* subverts innate immunity by dampening IL-1β and HMGB1 release during infection in GECs, *A. actinomycetemcomitans* can stimulate IL-6 and TNF-α production in BMDMs [54,68]. Likewise, infection with *F. nucleatum* stimulates cytokine production through the activation of Toll-like receptor (TLR)-2 and TLR-4 [54,69,70], or alternatively, through TLR-independent pathways [70,71]. Our results show that *F. nucleatum*-infected mice upregulate IL-1β, IL-6, TNF-α, and HMGB1, consistent with previous *in vitro* studies on GECs and BMDMs infected with *F. nucleatum* [46,54].

Given the heightened inflammatory response induced by *F. nucleatum* infection, it was not surprising to see a recruitment

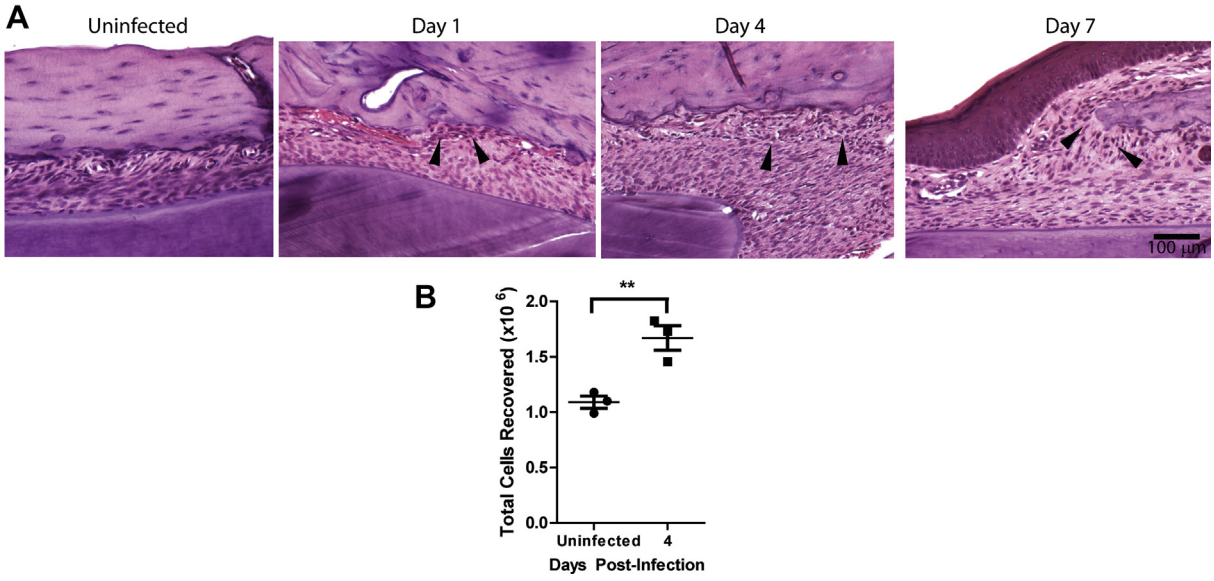

Fig. 4 **Immune cells are recruited near the alveolar bone during *F. nucleatum* infection**. (A) Sections from mandible of infected BALB/c mice were stained with H&E. Arrows indicate area of immune cells localized near the bone in dark stain. Bar represents 100 μm. (B) Total immune cells recruited to the murine gingival tissue of *F. nucleatum*-infected BALB/c mice at day 4. Graph shows mean ± SD of immune cell numbers found in the murine gingival tissue of infected mice. Results show an average of 6 mice in each group (**<0.01, Student's *t*-test).

of immune cells to the alveolar bone during infection. Macrophages are known to reside in dental pulp [72]. Their activation relies on exposure to IFN-γ, TNF-α, and LPS [73–75]. IFN-γ is important for antibacterial activity and is augmented by stimulation with LPS [76–78]. We found that *F. nucleatum* infection induced significant levels of IFN-γ. In addition, immunohistochemistry revealed the recruitment of macrophages throughout the oral cavity.

It remains to be determined whether IFN-γ promotes or inhibits osteoclast activation [39,62,79,80]. However, in our

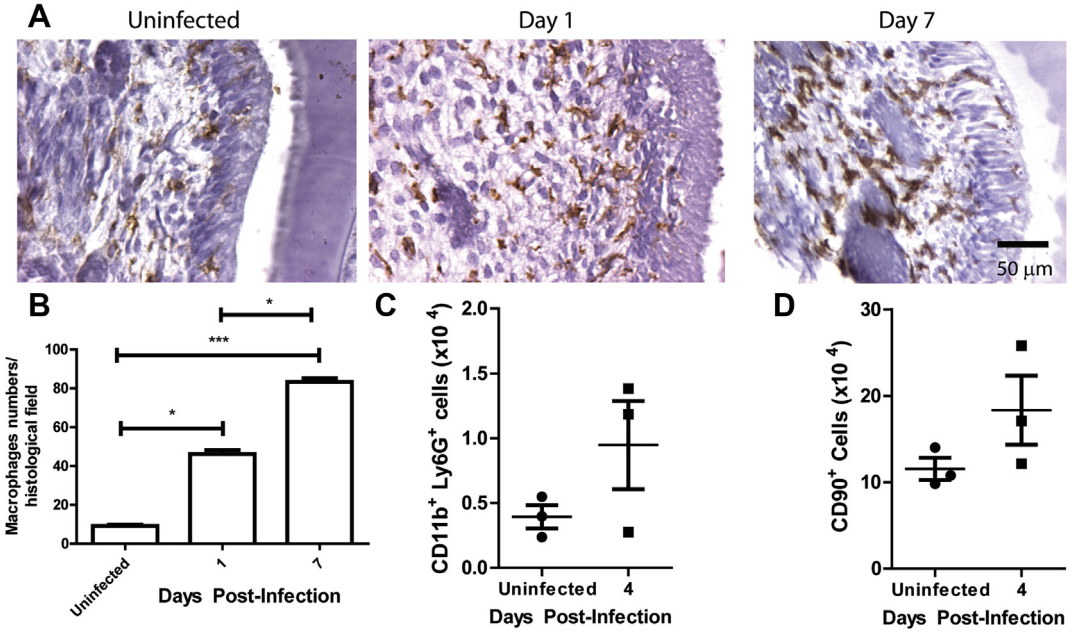

Fig. 5 ***F. nucleatum* infection increases immune cell recruitment in the dental pulp and in gingival tissue**. (A) Immunohistochemistry for F4/80^{+} macrophages in the dental pulp of infected BALB/c mice. Bar represents 50 μm. (B) Quantification of macrophages from 10 histological fields. Total (C) neutrophils (CD11b^{+} Ly6G^{+}) and (D) lymphocytes (CD90^{+}) recruited to the murine gingival tissue of *F. nucleatum*-infected BALB/c mice at day 4. Graphs show the mean ± SD of immune cells numbers found in the murine gingival tissue of infected or uninfected mice. (C and D) each point represents 2 mice in each group. Error bars represent the mean ± SD. (*<0.05, ***<0.001, Student's *t*-test).

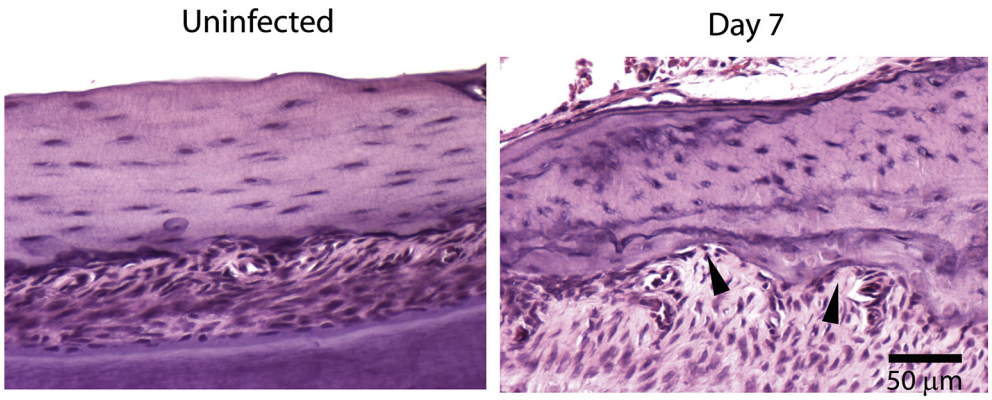

Fig. 6 **F. *nucleatum* infection induces bone resorption**. Mandibles of infected BALB/c mice were stained with H&E. Arrows indicate areas of bone resorption. Bar represents 50 μm.

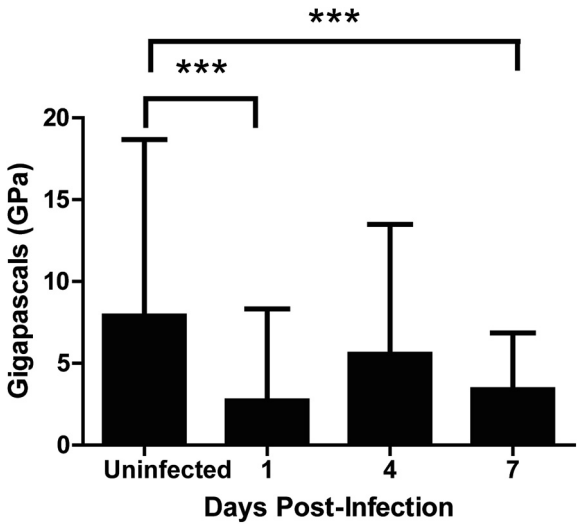

Fig. 7 **Alveolar bone is more elastic in *F. nucleatum*-infected mice**. Young modulus of alveolar bone was measured with an atomic force microscope. Results represent an average of at least 160 measurements from 4 different mice per group. Error bars represent the mean ± SD. Multiple comparisons were corrected with Dunnett's method.

study, IFN-γ may have contributed to activation of osteoclasts as they were observed localized near the bone after *F. nucleatum* infection. Moreover, TNF-α and IL-17 synergize with IL-1β, and can facilitate osteoclast activation, further supporting a role for these cytokines in bone loss in the mandible [81,82] during infection with *F. nucleatum*.

Conflicts of interest

The authors declare that they have no conflicts of interest.

Acknowledgements

This study was supported by intramural funds from the University of the Pacific, and the Fundação de Amparo à Pesquisa do Estado do Rio de Janeiro (FAPERJ). Cássio Luiz Coutinho Almeida-da-Silva received a PhD fellowship from CNPq (141715/2014-6) and FAPERJ (200417/2016; 200092/2016). Gustavo Miranda Rocha received a Postdoctoral fellowship from FAPERJ (217689/2015-2). We are grateful to Dr. Ana Morandini (University of the Pacific) for helpful discussions during preparation of this manuscript.

Appendix A. Supplementary data

Supplementary data related to this article can be found at https://doi.org/10.1016/j.bj.2018.05.001.

REFERENCES

[1] Dewhirst FE, Chen T, Izard J, Paster BJ, Tanner AC, Yu WH, et al. The human oral microbiome. J Bacteriol 2010;192:5002–17.
[2] Bik EM, Long CD, Armitage GC, Loomer P, Emerson J, Mongodin EF, et al. Bacterial diversity in the oral cavity of 10 healthy individuals. ISME J 2010;4:962–74.
[3] Han YW, Shi W, Huang GT, Kinder Haake S, Park NH, Kuramitsu H, et al. Interactions between periodontal bacteria and human oral epithelial cells: Fusobacterium nucleatum adheres to and invades epithelial cells. Infect Immun 2000;68:3140–6.
[4] Signat B, Roques C, Poulet P, Duffaut D. Fusobacterium nucleatum in periodontal health and disease. Curr Issues Mol Biol 2011;13:25–36.
[5] Armitage GC. Periodontal diagnoses and classification of periodontal diseases. Periodontology 2004;34:9–21.
[6] Silva N, Abusleme L, Bravo D, Dutzan N, Garcia-Sesnich J, Vernal R, et al. Host response mechanisms in periodontal diseases. J Appl Oral Sci: Revista FOB 2015;23:329–55.
[7] Arigbede AO, Babatope BO, Bamidele MK. Periodontitis and systemic diseases: a literature review. J Indian Soc Periodontol 2012;16:487–91.
[8] Hasan A, Palmer RM. A clinical guide to periodontology: pathology of periodontal disease. Br Dent J 2014;216:457–61.
[9] Karpathy SE, Qin X, Gioia J, Jiang H, Liu Y, Petrosino JF, et al. Genome sequence of Fusobacterium nucleatum subspecies polymorphum – a genetically tractable fusobacterium. PLoS One 2007;2:e659.

[10] Al-Ahmad A, Wunder A, Auschill TM, Follo M, Braun G, Hellwig E, et al. The in vivo dynamics of Streptococcus spp., Actinomyces naeslundii, Fusobacterium nucleatum and Veillonella spp. in dental plaque biofilm as analysed by five-colour multiplex fluorescence in situ hybridization. J Med Microbiol 2007;56:681–7.
[11] Zilm PS, Rogers AH. Co-adhesion and biofilm formation by Fusobacterium nucleatum in response to growth pH. Anaerobe 2007;13:146–52.
[12] Han YW, Ikegami A, Rajanna C, Kawsar HI, Zhou Y, Li M, et al. Identification and characterization of a novel adhesin unique to oral fusobacteria. J Bacteriol 2005;187:5330–40.
[13] Tuttle RS, Strubel NA, Mourad J, Mangan DF. A non-lectin-like mechanism by which Fusobacterium nucleatum 10953 adheres to and activates human lymphocytes. Oral Microbiol Immunol 1992;7:78–83.
[14] Mangan DF, Novak MJ, Vora SA, Mourad J, Kriger PS. Lectinlike interactions of Fusobacterium nucleatum with human neutrophils. Infect Immun 1989;57:3601–11.
[15] Temoin S, Wu KL, Wu V, Shoham M, Han YW. Signal peptide of FadA adhesin from Fusobacterium nucleatum plays a novel structural role by modulating the filament's length and width. FEBS Lett 2012;586:1–6.
[16] Xu M, Yamada M, Li M, Liu H, Chen SG, Han YW. FadA from Fusobacterium nucleatum utilizes both secreted and nonsecreted forms for functional oligomerization for attachment and invasion of host cells. J Biol Chem 2007;282:25000–9.
[17] Martinon F, Burns K, Tschopp J. The inflammasome: a molecular platform triggering activation of inflammatory caspases and processing of proIL-beta. Mol Cell 2002;10:417–26.
[18] Ozaki M, Miyake Y, Shirakawa M, Takemoto T, Okamoto H, Suginaka H. Binding specificity of Fusobacterium nucleatum to human erythrocytes, polymorphonuclear leukocytes, fibroblasts, and HeLa cells. J Periodontal Res 1990;25:129–34.
[19] Diamond G, Ryan L. Beta-defensins: what are they really doing in the oral cavity? Oral Dis 2011;17:628–35.
[20] Mathews M, Jia HP, Guthmiller JM, Losh G, Graham S, Johnson GK, et al. Production of beta-defensin antimicrobial peptides by the oral mucosa and salivary glands. Infect Immun 1999;67:2740–5.
[21] Dale BA, Krisanaprakornkit S. Defensin antimicrobial peptides in the oral cavity. J Oral Pathol Med : Off Publ Int Assoc Oral Pathol Am Acad Oral Pathol 2001;30:321–7.
[22] Gomes Pde S, Fernandes MH. Defensins in the oral cavity: distribution and biological role. J Oral Pathol Med: Off Publ Int Assoc Oral Pathol Am Acad Oral Pathol 2010;39:1–9.
[23] Rao MR, Preethi PL, Sathish M, Madhusudhan P. Gingival epithelial cell responses to microbial infections – an overview. J Res Adv Dent 2014;3:53–6.
[24] Dale BA. Periodontal epithelium: a newly recognized role in health and disease. Periodontology 2002;30:70–8.
[25] Laube DM, Dongari-Bagtzoglou A, Kashleva H, Eskdale J, Gallagher G, Diamond G. Differential regulation of innate immune response genes in gingival epithelial cells stimulated with Aggregatibacter actinomycetemcomitans. J Periodontal Res 2008;43:116–23.
[26] Medzhitov R. Toll-like receptors and innate immunity. Nat Rev Immunol 2001;1:135–45.
[27] Kawai T, Akira S. Signaling to NF-kappaB by Toll-like receptors. Trends Mol Med 2007;13:460–9.
[28] Kelk P, Claesson R, Chen C, Sjostedt A, Johansson A. IL-1beta secretion induced by Aggregatibacter (Actinobacillus) actinomycetemcomitans is mainly caused by the leukotoxin. Int J Medical Microbiol: IJMM 2008;298:529–41.
[29] Hung SC, Huang PR, Almeida-da-Silva CLC, Atanasova KR, Yilmaz O, Ojcius DM. NLRX1 modulates differentially NLRP3 inflammasome activation and NF-kappaB signaling during Fusobacterium nucleatum infection. Microbes Infect 2017:1–11, https://doi.org/10.1016/j.micinf.2017.09.014 [Epub ahead of print].
[30] Bui FQ, Johnson L, Roberts J, Hung SC, Lee J, Atanasova KR, et al. Fusobacterium nucleatum infection of gingival epithelial cells leads to NLRP3 inflammasome-dependent secretion of IL-1β and the danger signals ASC and HMGB1. Cell Microbiol 2016;18:970–81.
[31] Griffin GK, Newton G, Tarrio ML, Bu DX, Maganto-Garcia E, Azcutia V, et al. IL-17 and TNF-alpha sustain neutrophil recruitment during inflammation through synergistic effects on endothelial activation. J Immunol 2012;188:6287–99.
[32] McGee DW, Bamberg T, Vitkus SJ, McGhee JR. A synergistic relationship between TNF-alpha, IL-1 beta, and TGF-beta 1 on IL-6 secretion by the IEC-6 intestinal epithelial cell line. Immunology 1995;86:6–11.
[33] Guilloteau K, Paris I, Pedretti N, Boniface K, Juchaux F, Huguier V, et al. Skin inflammation induced by the synergistic action of IL-17A, IL-22, Oncostatin M, IL-1{alpha}, and TNF-{alpha} recapitulates some features of psoriasis. J Immunol 2010;184:5263–70.
[34] Awane M, Andres PG, Li DJ, Reinecker HC. NF-kappa B-inducing kinase is a common mediator of IL-17-, TNF-alpha-, and IL-1 beta-induced chemokine promoter activation in intestinal epithelial cells. J Immunol 1999;162:5337–44.
[35] Palmqvist P, Lundberg P, Lundgren I, Hanstrom L, Lerner UH. IL-1beta and TNF-alpha regulate IL-6-type cytokines in gingival fibroblasts. J Dental Res 2008;87:558–63.
[36] Saperstein S, Chen L, Oakes D, Pryhuber G, Finkelstein J. IL-1beta augments TNF-alpha-mediated inflammatory responses from lung epithelial cells. J Interferon Cytokine Res: Off J Int Soc Interferon Cytokine Res 2009;29:273–84.
[37] Vignery A, Baron R. Dynamic histomorphometry of alveolar bone remodeling in the adult rat. Anat Rec 1980;196:191–200.
[38] Hienz SA, Paliwal S, Ivanovski S. Mechanisms of bone resorption in periodontitis. J Immunol Research 2015;2015:615486.
[39] Soysa NS, Alles N, Aoki K, Ohya K. Osteoclast formation and differentiation: an overview. J Med Dent Sci 2012;59:65–74.
[40] Goltzman D. Discoveries, drugs and skeletal disorders. Nat Rev 2002;1:784–96.
[41] Boyce BF, Li P, Yao Z, Zhang Q, Badell IR, Schwarz EM, et al. TNF-alpha and pathologic bone resorption. Keio J Med 2005;54:127–31.
[42] Hwang SY, Putney Jr JW. Calcium signaling in osteoclasts. Biochim Biophys Acta 2011;1813:979–83.
[43] Blair HC, Robinson LJ, Zaidi M. Osteoclast signalling pathways. Biochem Biophys Res Commun 2005;328:728–38.
[44] Hayman AR. Tartrate-resistant acid phosphatase (TRAP) and the osteoclast/immune cell dichotomy. Autoimmunity 2008;41:218–23.
[45] Lee HR, Rhyu IC, Kim HD, Jun HK, Min BM, Lee SH, et al. In-vivo-induced antigenic determinants of Fusobacterium nucleatum subsp. nucleatum. Mol Oral Microbiol 2011;26:164–72.
[46] Bui FQ, Johnson L, Roberts J, Hung SC, Lee J, Atanasova KR, et al. Fusobacterium nucleatum infection of gingival epithelial cells leads to NLRP3 inflammasome-dependent secretion of IL-1beta and the danger signals ASC and HMGB1. Cell Microbiol 2016;18:970–81.
[47] Kostic AD, Chun E, Robertson L, Glickman JN, Gallini CA, Michaud M, et al. Fusobacterium nucleatum potentiates intestinal tumorigenesis and modulates the tumor-immune microenvironment. Cell Host Microbe 2013;14:207–15.

[48] Dharmani P, Strauss J, Ambrose C, Allen-Vercoe E, Chadee K. Fusobacterium nucleatum infection of colonic cells stimulates MUC2 mucin and tumor necrosis factor alpha. Infect Immun 2011;79:2597–607.
[49] Zaborina O, Li X, Cheng G, Kapatral V, Chakrabarty AM. Secretion of ATP-utilizing enzymes, nucleoside diphosphate kinase and ATPase, by Mycobacterium bovis BCG: sequestration of ATP from macrophage P2Z receptors? Mol Microbiol 1999;31:1333–43.
[50] Baker PJ, Dixon M, Evans RT, Roopenian DC. Heterogeneity of Porphyromonas gingivalis strains in the induction of alveolar bone loss in mice. Oral Microbiol Immunol 2000;15:27–32.
[51] Mizraji G, Segev H, Wilensky A, Hovav AH. Isolation, processing and analysis of murine gingival cells. JoVE 2013;77: e50388.
[52] Ramos-Junior ES, Morandini AC, Almeida-da-Silva CL, Franco EJ, Potempa J, Nguyen KA, et al. A dual role for P2X7 receptor during Porphyromonas gingivalis infection. J Dental Res 2015;94:1233–42.
[53] Liu P, Liu Y, Wang J, Guo Y, Zhang Y, Xiao S. Detection of fusobacterium nucleatum and fadA adhesin gene in patients with orthodontic gingivitis and non-orthodontic periodontal inflammation. PLoS One 2014;9:e85280.
[54] Park SR, Kim DJ, Han SH, Kang MJ, Lee JY, Jeong YJ, et al. Diverse Toll-like receptors mediate cytokine production by Fusobacterium nucleatum and Aggregatibacter actinomycetemcomitans in macrophages. Infect Immun 2014;82:1914–20.
[55] Andersson U, Erlandsson-Harris H, Yang H, Tracey KJ. HMGB1 as a DNA-binding cytokine. J Leukoc Biol 2002;72:1084–91.
[56] Lotze MT, Tracey KJ. High-mobility group box 1 protein (HMGB1): nuclear weapon in the immune arsenal. Nat Rev Immunol 2005;5:331–42.
[57] Erlandsson Harris H, Andersson U. Mini-review: the nuclear protein HMGB1 as a proinflammatory mediator. Eur J Immunol 2004;34:1503–12.
[58] Kalinina N, Agrotis A, Antropova Y, DiVitto G, Kanellakis P, Kostolias G, et al. Increased expression of the DNA-binding cytokine HMGB1 in human atherosclerotic lesions: role of activated macrophages and cytokines. Arterioscler Thromb Vasc Biol 2004;24:2320–5.
[59] Lam RS, O'Brien-Simpson NM, Lenzo JC, Holden JA, Brammar GC, Walsh KA, et al. Macrophage depletion abates Porphyromonas gingivalis-induced alveolar bone resorption in mice. J Immunol 2014;193:2349–62.
[60] Vaananen K. Mechanism of osteoclast mediated bone resorption–rationale for the design of new therapeutics. Adv Drug Deliv Rev 2005;57:959–71.
[61] Teitelbaum SL. Bone resorption by osteoclasts. Science 2000;289:1504–8.
[62] Gao Y, Grassi F, Ryan MR, Terauchi M, Page K, Yang X, et al. IFN-gamma stimulates osteoclast formation and bone loss in vivo via antigen-driven T cell activation. J Clin Investig 2007;117:122–32.
[63] Zupan J, Jeras M, Marc J. Osteoimmunology and the influence of pro-inflammatory cytokines on osteoclasts. Biochem Med 2013;23:43–63.
[64] Diaz PI, Zilm PS, Rogers AH. Fusobacterium nucleatum supports the growth of Porphyromonas gingivalis in oxygenated and carbon-dioxide-depleted environments. Microbiology 2002;148:467–72.
[65] Saito Y, Fujii R, Nakagawa KI, Kuramitsu HK, Okuda K, Ishihara K. Stimulation of Fusobacterium nucleatum biofilm formation by Porphyromonas gingivalis. Oral Microbiol Immunol 2008;23:1–6.
[66] Periasamy S, Kolenbrander PE. Aggregatibacter actinomycetemcomitans builds mutualistic biofilm communities with Fusobacterium nucleatum and Veillonella species in saliva. Infect Immun 2009;77:3542–51.
[67] Metzger Z, Lin YY, Dimeo F, Ambrose WW, Trope M, Arnold RR. Synergistic pathogenicity of Porphyromonas gingivalis and Fusobacterium nucleatum in the mouse subcutaneous chamber model. J Endod 2009;35:86–94.
[68] Johnson L, Atanasova KR, Bui PQ, Lee J, Hung SC, Yilmaz O, et al. Porphyromonas gingivalis attenuates ATP-mediated inflammasome activation and HMGB1 release through expression of a nucleoside-diphosphate kinase. Microbes Infect 2015;17:369–77.
[69] Toussi DN, Liu X, Massari P. The FomA porin from Fusobacterium nucleatum is a Toll-like receptor 2 agonist with immune adjuvant activity. Clin Vaccine Immunol 2012;19:1093–101.
[70] Liu H, Redline RW, Han YW. Fusobacterium nucleatum induces fetal death in mice via stimulation of TLR4-mediated placental inflammatory response. J Immunol 2007;179:2501–8.
[71] Quah SY, Bergenholtz G, Tan KS. Fusobacterium nucleatum induces cytokine production through Toll-like-receptor-independent mechanism. Int Endod J 2014;47:550–9.
[72] Iwasaki Y, Otsuka H, Yanagisawa N, Hisamitsu H, Manabe A, Nonaka N, et al. In situ proliferation and differentiation of macrophages in dental pulp. Cell Tissue Res 2011;346:99–109.
[73] Mosser DM, Zhang X. Activation of murine macrophages. In: Coligan John E, et al., editors. Current protocols in immunology; 2008 [Chapter 14:Unit 14 2].
[74] Mosser DM, Edwards JP. Exploring the full spectrum of macrophage activation. Nat Rev Immunol 2008;8:958–69.
[75] Mosser DM. The many faces of macrophage activation. J Leukoc Biol 2003;73:209–12.
[76] Schroder K, Hertzog PJ, Ravasi T, Hume DA. Interferon-gamma: an overview of signals, mechanisms and functions. J Leukoc Biol 2004;75:163–89.
[77] Kamijo R, Le J, Shapiro D, Havell EA, Huang S, Aguet M, et al. Mice that lack the interferon-gamma receptor have profoundly altered responses to infection with Bacillus Calmette-Guerin and subsequent challenge with lipopolysaccharide. J Exp Med 1993;178:1435–40.
[78] Shtrichman R, Samuel CE. The role of gamma interferon in antimicrobial immunity. Curr Opin Microbiol 2001;4:251–9.
[79] Takayanagi H, Ogasawara K, Hida S, Chiba T, Murata S, Sato K, et al. T-cell-mediated regulation of osteoclastogenesis by signalling cross-talk between RANKL and IFN-gamma. Nature 2000;408:600–5.
[80] Boyle WJ, Simonet WS, Lacey DL. Osteoclast differentiation and activation. Nature 2003;423:337–42.
[81] Yago T, Nanke Y, Ichikawa N, Kobashigawa T, Mogi M, Kamatani N, et al. IL-17 induces osteoclastogenesis from human monocytes alone in the absence of osteoblasts, which is potently inhibited by anti-TNF-alpha antibody: a novel mechanism of osteoclastogenesis by IL-17. J Cell Biochem 2009;108:947–55.
[82] Kotake S, Udagawa N, Takahashi N, Matsuzaki K, Itoh K, Ishiyama S, et al. IL-17 in synovial fluids from patients with rheumatoid arthritis is a potent stimulator of osteoclastogenesis. J Clin Investig 1999;103:1345–52.